Radiation control in deuterium, tritium and deuterium-tritium JET baseline plasmas – part I

L. Piron [a,b,*], D. Van Eester [c], D. Frigione [d], L. Garzotti [e], P.J. Lomas [e], M. Lennholm [e], F. Rimini [e], F. Auriemma [b], M. Baruzzo [d], P.J. Carvalho [f], D.R. Ferreira [f], A.R. Field [e], K. Kirov [e], Z. Stancar [e], C.I. Stuart [e], D. Valcarcel [e], JET Contributors[1]

[a] *Dipartimento di Fisica "G. Galilei", Università degli Studi di Padova, Padova, Italy*
[b] *Consorzio RFX, Corso Stati Uniti 4, Padova, Italy*
[c] *Laboratory for Plasma Physics LPP-ERK/KMS, Bruxelles, Belgium*
[d] *ENEA, Fusion and Nuclear Safety Department, C.R. Frascati, Rome, Italy*
[e] *CCFE, Culham Science Centre, Abingdon OX14 3DB, United Kingdom*
[f] *Instituto de Plasmas e Fusão Nuclear, Instituto Superior Técnico Universidade de Lisboa 1049-001, Lisboa, Portugal*

The achievement of a steady ELMy H-mode phase with high ion temperature, but without a gradual rise in plasma radiation, has been a crucial point to establish high plasma performance scenarios in JET ITER-like-wall plasmas. Indeed, radiation events, due to the release of high Z impurities, such as Nickel and Copper, and W sputtered from the divertor, can strongly reduce the power crossing the plasma separatrix and slow the ELMs dynamics, thus inducing H to L transition. In particular, in JET baseline plasmas, because of the outward neo-classical transport [A.R. Field et al 2021 Plasma Phys. Control. Fusion 63 095013], plasma impurities are mainly localized in the mantle region, as detected by a real-time surrogate model for bolometer tomography based on machine learning [D.R. Ferreira et al 2021 Fusion Engineering and Design 164], and the consequent excessive radiation in this region is the main cause of plasma termination in recent Deuterium, Tritium and Deuterium-Tritium operations. To guarantee impurity accumulation being flushed by the ELMs, ELM control schemes, which ensure a throughput of particles, either via gas fueling and via pellets, have been exploited. In this work, the staged approach strategy towards radiation control, which allowed to sustain for more than 10 s Tritium and Deuterium-Tritium baseline discharges without radiation issues, is presented.

1. Introduction

In 2020/2021, JET offered the unique opportunity to study the behavior of Tritium (T) and Deuterium-Tritium (DT) plasmas in conditions and dimensions approaching those required in ITER (DTE2) [1]. With respect to the first DT campaign in 1997 (DTE1) [2], when JET was equipped with a Carbon wall, the experiments have been performed with a Tungsten (W) divertor and a Beryllium first wall, with a higher total auxiliary power and an improved coverage of diagnostics.

In preparation to DTE2, an intense activity of scenario development has been embarked in Deuterium to prepare the plasmas needed to demonstrate stationary high fusion performance [3] and a pure Tritium campaign has been conducted to assess how the isotopic effects affect the plasma scenarios developed, complementing the previous Hydrogen campaign studies [4].

The main challenge that has been faced at JET with the new wall, if the frequency of ELMs (edge localized mode) becomes too low, is the risk of having plasmas polluted by high Z impurities, such as Nickel and Copper, due to NBI duct scraper and Ni to ICRH limiters, respectively, and W sputtered from the divertor, which can cause radiation events [5], and thus plasma disruptions.

To avoid these events, low particle throughput has to be achieved by a proper control of ELM frequency. Over the years, various ELM control strategies have been developed and tested in JET baseline plasmas in preparation to DTE2 [6–8] which rely on: i) vertical kicks, which consist in a rapid vertical plasma movement, by changing the radial magnetic field, ii) gas fuelling, and iii) injection of pellets of frozen hydrogenic isotopes into the plasma.

Vertical kicks are not suitable for the high plasma current operations foreseen in DTE2 because of the associated risk of vertical displacement events. Gas flow alone is also not effective. High levels of gas are indeed requested to maintain ELM frequency as desired, which lead to plasma confinement degradation and hence performance reduction. The optimal ELM control strategy consists of using a combination of gas fuelling and ELM-pacing pellets. This is the control strategy adopted in T and DT baseline plasmas at Ip=3.5 MA, B_t= 3.25 T that are described in this paper.

The control of radiation has been challenging in T and DT. Indeed, the ELM frequency was lower in T than in D and the initial ELM-free phase was longer, as observed in DTE1 [9], and predicted by modelling [10]. In T and DT pulses, the Tritium Introduction Modules (TIMs) have been used to fuel the plasma with T. These valves, differently to the Gas Introduction Modules, used to fuel D, have a delayed response of about 200 ms, and this makes ELM control even more difficult.

Hence, a staged approach has been adopted to identify the best settings of the ELM control actuators, i.e. gas flow and pellet injector, to guarantee an efficient flush of impurities from the plasma.

In this work, the approach to radiation control is reported, considering a database of JET T and DT baseline plasmas with Ip=3.5 MA. In particular, Section 2 reports the lessons learned on radiation control from D operations. Section 3 summarizes the optimization of ELM control, which allows to sustain a T and DT discharge with 33 MW auxiliary power (PNBI=29 MW+ PICRH =4MW) up to 10.2 s and 11 s, respectively, without radiation issues. Section 4 gives the conclusions.

2. Lesson learnt from Deuterium operation

Excessive radiation has been the main cause of stop (e.g. the first event that triggers a controlled plasma termination) in JET D baseline plasmas, with a rate of 43%. Radiation runaway events are due the presence of high Z impurities and sputtered W from the divertor, which are not flushed out from the confined plasma but are mainly localized in the low-field side (LFS) region because of the outward neoclassical transport convention [10].

Radiation is monitored in JET by two systems:

(i) the real-time control system, where several metrics are calculated by the Real Time Central Controller (RTCC), such as the radiation fraction, which is the ratio between the total radiation as measured by the vertical bolometer fan [11] and the total input power, and bolometry peaking, defined as the ratio between a central and an off axis bolometer channel.

(ii) the Plasma Event TRiggering for Alarm (PETRA) system [12], where a surrogate model for bolometer tomography reconstruction based on machine-learning has been deployed [13] and offers the possibility of monitoring the radiated power in specific regions of interest, such as the LFS, where impurities tend to accumulate in baseline plasmas [9], and the core region, named here $P_{rad\ LFS}$ and $P_{rad\ core}$, respectively.

Since the plasma performance cannot recover from a radiation runaway event, as radiation metrics exceed certain thresholds, a controlled termination of the pulse, called jump to termination (JTT), is initiated.

To avoid a radiation collapse, it is of paramount importance to avoid heavy impurity accumulation. The experience that has been capitalized from D operation is that the combination of ELM pacing pellets + gas fuelling promotes the removal of impurities by means of ELMs.

This is demonstrated in Fig. 1 which shows a pair of I_p=3.5 MA, B_t=3.25 T Deuterium discharges where two strategies for ELM control have been compared: only gas fuelling, in the pulse plotted in blue, pellets + gas fuelling, in the pulse in red. In particular, the train of ELM pacing pellets has been programmed at a repetition frequency of 45 Hz, in the time interval t=[7.55–8.5] s, then 35 Hz.
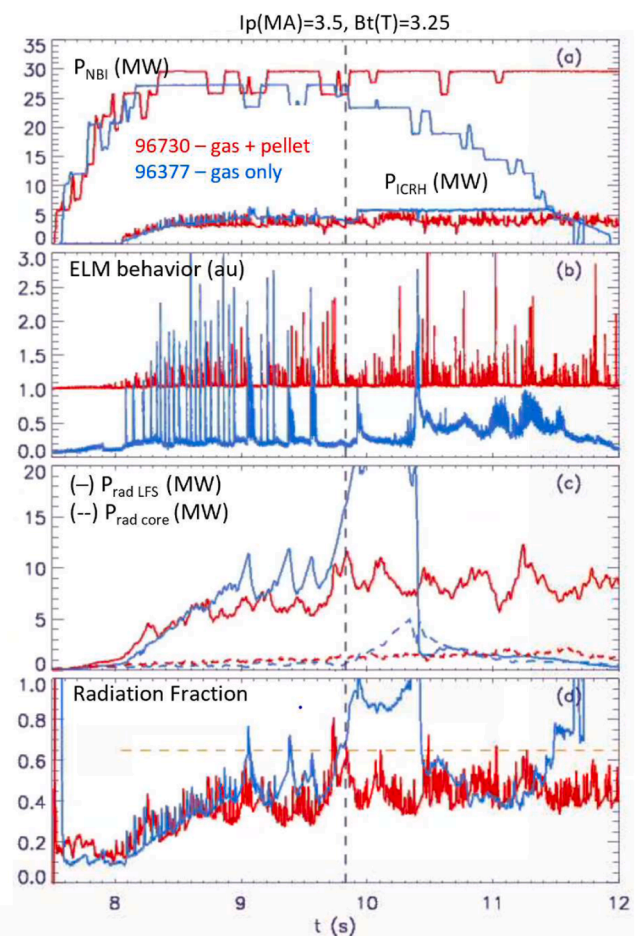

Fig. 1. Time behavior of (a) auxiliary heating power, (b) ELMs, (c) radiation in the core (dotted line) and in the LFS (solid line) as calculated by bolometer tomography based on machine learning and (d) radiation fraction in a pair of I_p=3.5 MA, B_t=3.25 T Deuterium discharges. ELM dynamics is controlled by only gas fuelling in the discharge plotted in blue, and pellet+gas fuelling in the discharge in red. The vertical dotted line corresponds to the time instant of stop while the orange dotted line indicates the threshold on radiation fraction set in JET real-time control system.

In the gas only fuelled pulse, as shown in Fig. 1(b), after the L-H transition, regular type-I ELMs can be observed, but from t=9 s, the ELMs are less reliably triggered, and there are periods of ELM free phases. This causes heavy impurities to not being flushed anymore, until the 0.65 empirically-tuned threshold on radiation fraction has been reached at around t=9.83 s, which initiates JTT. On the other hand, in the pellet + gas fuelled pulse, erratic type-I ELMs with a compound character have been triggered, which guaranteed a good flushing level of impurities and thus no radiation building up has been encountered through all the plasma phase.

It is worth mentioning that the pellet + gas fuelling recipe not only prevents radiation building up, but also corresponds to a lower total fuelling rate, with a part of the gas fuelling being replaced with the injection of pellets. This allows for a more modest deterioration of the confinement than with gas fuelling alone [3].

3. The path of radiation control in tritium and deuterium-tritium

The experience gained from D operation suggests using ELM-pacing pellets + gas fuelling to avoid radiation runaway events.

However, it has not been possible to apply straightforwardly such control scheme into T and DT plasmas because of isotope physics and

operation related aspects. Indeed, in T and in DT, the dynamic of ELMs was slower than in D and the ELM free phase lasted longer. This was compounded by the different behavior of Tritium injection modules (TIMs) with respect to gas injection modules (GIMs), and by the gas species itself. Therefore, the control of radiation has followed a staged approach, which envisaged the identification of the optimal settings in the pellet + gas fuelling scheme. It is worth highlighting that such identification has been hampered by stringent limitations on the experimental time available, on T consumption, and neutron activation (in Deuterium-Tritium).

The path to radiation control is described in the following sub-sections, presenting baseline plasmas with 3.5 MA plasma current (I_p) and 3.25 toroidal magnetic field (B_t). In these experiments, the radiation level has been monitored continuously 0.5 s after the NBI injection, by a series of radiation metrics available in JET real-time control and PETRA systems.

3.1. Radiation control in tritium

To guarantee flushing of impurities and thus avoid radiation from building up, gas fuelling and pellet injector settings have to be tuned when operating in Tritium.

The level of gas flow has been chosen, based on the response of GIMs [8], to achieve a density level, and thus an H mode entry, similar to the D one. Regarding the injection of pellets, 2 mm Hydrogen pellets have been launched from a flight line located at the upper high-field side of the main vessel [12]. The pellet injection time and frequency have been scanned with the aim of delaying the radiation from building up.

In the first T baseline attempt at I_p=3.5 MA, reported in blue in Fig. 2, Hydrogen pellets at a 25 Hz requested frequency have been injected from t=8.5 s. Initially, the threshold for radiation fraction limit had been set to 0.6, because of the uncertainty on the ELM behaviour while using T. The plasma transited to H mode at around t=7.75 s, as shown in Fig. 2 (b), but ELMs have been sporadically triggered. This induced radiation runaway which was localized in the LFS, as indicated by the real-time tomographic bolometry metrics, reported in Fig. 2 (c). After the long ELM-free phase of duration ~0.2 s, the radiation power increased to more than 60% of the input power, as shown in Fig. 2 (d), at which point this triggered a controlled termination of the pulse, which commenced with a strong increase of the gas puffing rate (not shown).

To promote ELM triggering, the injection of pellets has been thus anticipated to t=7.55 s in the pulse plotted in green in the same figure. In this case, after the H mode entry, at around t=7.8 s, regular ELMs paced at 25 Hz have been triggered, as reported in Fig. 2 (b). However, an ELM free phase occurred, which was responsible for impurity accumulation, mainly in the LFS, and thus radiation building up. Similarly to the previous discharge, but with a 0.140 s delay, the JET real-time control system detected an excessive radiation fraction level in the plasma, above 60%, and initiated the pulse termination.

To prevent ELM free phases, the pellet injection rate has been increased from 25 Hz to 35 Hz in the time interval t=[7.55–8.75] s, and afterwards has been set at 17 Hz. These settings have been tested in the plasma plotted in red in Fig. 2. As shown in Fig. 2(b), these settings ameliorate the ELM dynamics resulting in higher frequency, higher amplitude ELMs which allowed to delay the radiation building up by t=1.5 s with respect to the previously described discharge. However, at around t=10 s, the empirically identified 15 MW threshold was reached by the $P_{rad\ LFS}$ metrics, as detected by PETRA system, which commenced the plasma termination. Note that in this discharge, because of the improved ELM control achieved, more relaxed radiation fraction limits, highlighted in the orange horizontal line in Fig. 2(d), have been used.

The ELM control settings used in this discharge are the optimal ones at present since they allowed to maintain radiation under control in a I_p=3.5 MA baseline plasmas with 33 MW input power up to t=10.2 s.

It is worth highlighting that not all the injected pellets triggered ELMs. This has been quantified by calculating the efficiency indicator
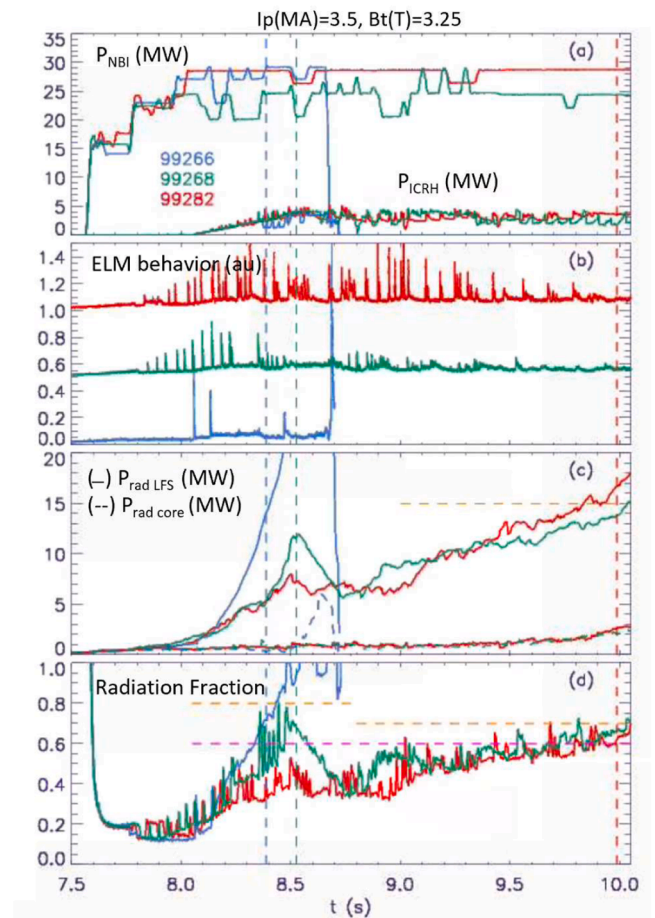
which is the ratio between the probability of an ELM being triggered by a pellet, based on a Bayesian approach described in [14], and the number of pellet injected within a time interval. The results of this analysis are shown in Fig. 3. The time intervals where the analysis has been carried out are represented with a dotted vertical line in the figure. Note that overall, the pellet injection settings used in the discharge plotted in red
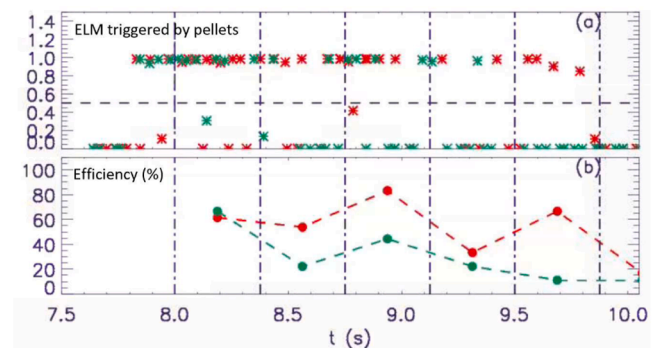

Fig. 2. Time behavior of (a) auxiliary heating power, (b) ELMs, (c) radiation in the core (dotted line) and in the LFS (solid line) as calculated by bolometer tomography based on machine learning and (d) radiation fraction in three I_p=3.5 MA, B_t=3.25 T Tritium discharges, which differ from pellet injection settings. The time of the stop is highlighted with a vertical dotted line. The horizontal magenta dotted line represents the radiation fraction limit adopted when firstly operating JET with T. Such a threshold has been relaxed afterwards, and set to higher value, as highlighted in orange.

Fig. 3. Time behavior of (a) the probability of an ELM being triggered by a pellet [12] and (b) pellet efficiency in triggering an ELM. Data corresponds to the set of discharges presented in Fig. 2.

in Fig. 2 resulted in an efficiency level on average above 50%, larger w.r.t the one in the pulse in green. Indeed, these optimal settings have guaranteed a good impurity flushing, delaying the radiation building up.

3.2. Radiation control in deuterium-tritium

Radiation control in DT operation, analogously to T operation, has followed a staged approach. In particular, a scan of pellet frequency and a scan of gas fuelling have been performed to identify the optimal settings in the ELM control actuators which can prevent impurity accumulation and thus the radiation collapse. It is worth highlighting that for controlling radiation, the same limits in the radiation fraction and LFS radiation metrics used in 99282 T discharge have been adopted.

The discharges presented in this section have an isotope mixture close to 50:50, which is the best ratio to promote fusion reactions. This isotope mixture composition has been achieved by carefully pre-programming the GIM and TIM flow rates taking into account the contributions of NBI and pellets to plasma fuelling.

Fig. 4 presents a series of DT discharges at $I_p=3.5$ MA, $B_t=3.25$ T where the gas flow has been tuned to achieve a density level at H mode entry similar to the D one and then has been set around 1×10^{22} (e/s) in the main heating phase. A similar level of particle throughput can be also achieved when injecting D pellets. The frequency of D pellet injection has been varied in these discharges: in the pulse plotted in green,

Fig. 4. Time behavior of (a) auxiliary heating power, (b) ELMs, (c) radiation in the core (dotted line) and in the LFS (solid line) as calculated by bolometer tomography based on machine learning and (d) radiation fraction in three of $I_p=3.5$ MA, $B_t=3.25$ T Deuterium-Tritium discharges, which differ from pellet injection frequency. The time of the stop is highlighted with a dotted vertical line.

the pellets have been injected from t=7.55s at 45 Hz, in the pulse plotted in blue, the same settings have been used up to t=8.5 s, but then, the pellet frequency has been reduced at 35 Hz. In the pulse plotted in red, because of the malfunction in the pellet injection, no pellets have been delivered to the plasma, so it can be counted as a gas-only fuelled pulse. This discharge is of particular interest because it shows the importance of a reliable pellet injection to avoid radiation runaway events. Indeed, without pellet injection, ELMs were sporadically triggered and an interval of ELM free phases occurred, which favored impurity accumulation and thus an exponential increase of radiation, which was detected at around t=8.5 s as the radiation fraction metrics reached the 80% level.

On the other hand, in both pulses with pellets successfully injected, as shown in Fig. 4(b), ELMs exhibited a complex behavior, with some large, type-I ELMs, each followed by a period of small ELMs before t=10 s. The efficiency of the pellets in triggering an ELM was in both the cases above 60% (not shown). However, after t=10 s, the ELM bursts have smaller amplitudes and the pellet efficiency starts to decrease. In this case, the impurity flushing necessary for the scenario to remain stationary is lost. Consequently, the radiation increased and a stop due to excessive radiation fraction, in the pulse plotted in blue, and excessive Prad in the LFS, in the plasma in green, have been detected by the JET real-time control system and the PETRA system, respectively. This happened around t=10.6 s, in both cases.

The similar behavior of radiation dynamics in these discharges suggests that the change of pellet frequency from 35 Hz to 45 Hz did not improve radiation control. This insight is also confirmed by a statistical analysis performed for the all DT database reported in [15].

As aforementioned, a gas fuelling scan has been also carried out in DT plasmas, while keeping the same 45 Hz pellet frequency from t=8.5 s, to assess its role in delaying the radiation from building up.

The results of such gas scan, which has been performed from t=9 s, are reported in Fig. 5. A colour code has been used here to distinguish the various gas flow levels (green corresponds to the lower gas rate, indicatively about 0.7×10^{22} e/s, blue to the medium gas rate, about 1×10^{22} e/s, and red to the higher gas rate, about 1.5×10^{22} e/s. The radiation, as shown in Fig. 5(c-d), slowly increased in time, up to a point in which the 15 MW threshold set in PETRA on $P_{rad\ LFS}$, has been reached. Note that such threshold was achieved later on as the gas flow level was increased. Actually, in the pulse plotted in red, the radiation has been maintained controlled up to t=11 s. This implies that the optimal gas fuelling rate is around 1.5×10^{22} (e/s), based on present knowledge.

The discharge where this gas fuelling rate has been tested had also a larger chance of having an ELM being triggered by a pellet. This is shown in Fig. 6 (b) where the calculation of pellet's efficiency in triggering ELMs is reported for the discharges with different gas flow rates.

4. Conclusion

This work summarized the main achievements obtained on radiation control during T and DT experiments in JET which took place in 2020/2021.

To monitor radiation evolution, a series of metrics were available in real-time, which have been calculated by programmable schemes using bolometric signals in the JET real-time control system, and derived by a surrogate model for bolometer tomography, based on machine learning, available in the brand-new PETRA system.

In DT and especially in T, the control of radiation per se has been challenging because of the different ELM dynamics with respect to D operation, the different behavior of GIMs with respect to TIMs, and the gas species itself. This has been also acerbated by the limited experimental time available and the restrictions imposed by T consumption and neutron activation (in DT).

In this context, a staged approach has been pursued to identify the optimal settings of gas dosing and pellet injection, which promote an
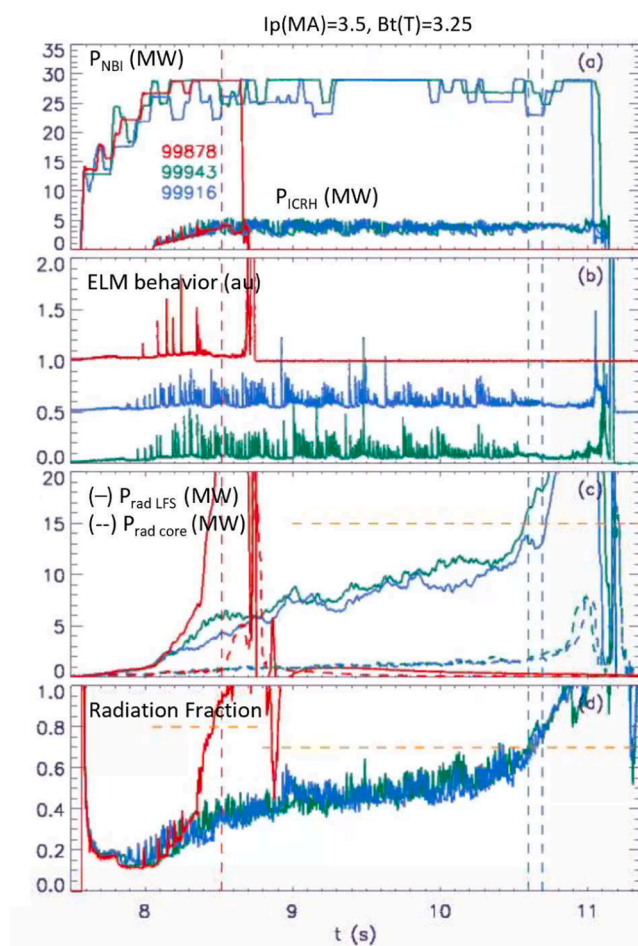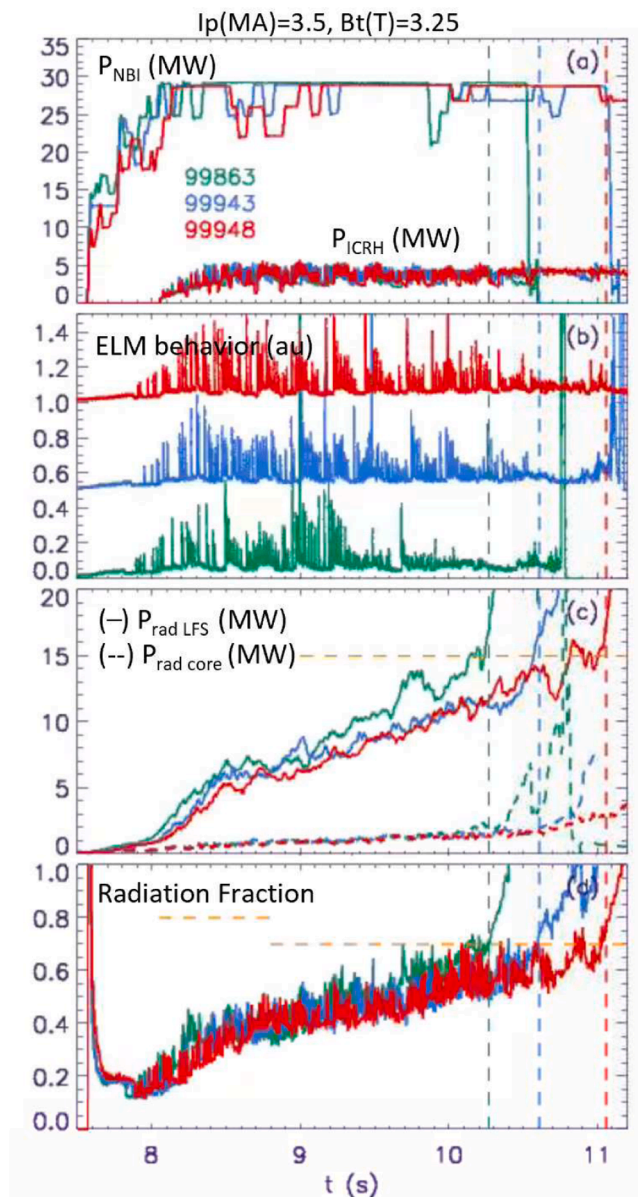
Fig. 5. Time behavior of (a) auxiliary heating power, (b) ELMs, (c) radiation in the core (dotted line) and in the LFS (solid line) as calculated by bolometer tomography based on machine learning and (d) radiation fraction in three I_p=3.5 MA, B_t=3.25 T Deuterium-Tritium discharges, which differ from the gas fuelling rate. The gas fuelling rate used is described in the text. The time of stop is highlighted with a dotted vertical line.

efficient impurity flushing by means of ELMs, while guarantying good plasma confinement properties.

The optimal settings for ELM control allow to sustain I_p=3.5 MA, B_t=3.35 T baseline T and DT discharges up to 10.2 s and 11 s, respectively, without radiation issues. Generally, the operation in T suffers from high levels of radiation, and hence, high impurity content. This can be due to different mechanisms, such as the increased sputtering due to the higher isotope mass [16], the development of hollow density profiles, which can affect plasma transport [15] and the different power threshold for the L to H transition in these plasmas.

The properties of the radiated power in T and DT plasma are still under investigation, and in particular the role of alpha particle population on particle transport and ELM stability. Once a deep knowledge is acquired, a further optimization of control schemes for radiation control will be carried out in preparation to DTE3 campaign. In particular, to
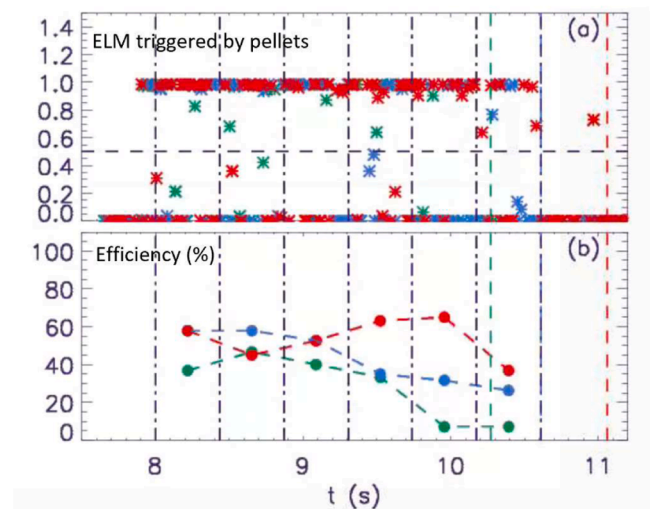

Fig. 6. Time behavior of (a) the probability of an ELM being triggered by a pellet [12] and (b) pellet efficiency in triggering an ELM. Data corresponds to the set of discharges presented in Fig. 5.

sustain longer DT baseline plasmas, to demonstrate fusion power up to 15 MW, sustained for 5 s, two possible strategies can be envisaged in DTE3, which rely on increased NBI power and/or the exploration of a lower plasma current regime. Both of these paths can guarantee a stationary and compound ELM dynamics, easing the radiation runaway issue.

Declaration of Competing Interest

The authors declare that they have no known competing financial interests or personal relationships that could have appeared to influence the work reported in this paper.

Data availability

Data will be made available on request.

Acknowledgments

References

[1] J. Mailloux, et al., Nucl. Fusion 62 (2022), 042026.
[2] M. Keilhacker, et al., Nucl. Fusion 39 (1999) 209.
[3] L. Garzotti, et al., Nucl. Fusion 59 (2019), 076037.
[4] C.F. Maggi, et al., Plasma Phys. Control. Fusion 60 (2018), 014045.
[5] A.R. Field, et al., Plasma Phys. Control. Fusion 63 (2021), 095013.
[6] F.G. Rimini, et al., Fusion Eng. Des. 86 (2011) 539–543.
[7] M. Lennholm, et al., Nucl. Fusion 55 (2015) 06300.
[8] L. Piron, et al., Fusion Eng. Des. 166 (2021), 112305.
[9] JET Team, Nucl. Fusion 39 (1999) 1875.
[10] S.E. Snyder, et al., Phys. of Plasmas 12 (2005), 112508.
[11] A. Huber, et al., J. Nucl. Mater. 363–365 (2007) 365–370.
[12] C.I. Stuart, et al., Fusion Eng. Des. 168 (2021), 112412.
[13] D.R. Ferreira, et al., Fusion Eng. Des. 164 (2021), 112179.
[14] M. Lennholm, et al., Nucl. Fusion 61 (2021), 036035.
[15] L. Piron et al statistics of radiation control in D,T,DT plasmas, paper in preparation.
[16] C. Guillemaut, et al., Phys. Scr. 2016 (2016), 014005.